Journal of Veterinary Diagnostic Investigation
2019, Vol. 31(6) 859–863

DOI: 10.1177/1040638719874857
jvdi.sagepub.com

Pancreatic Langerhans cell histiocytosis in a cat

Daniel R. Rissi,[1] Cathy A. Brown, Karine Gendron, Jennifer Good, Selena Lane, Chad W. Schmiedt

Abstract. In contrast to pulmonary Langerhans cell histiocytosis (LCH), which is a proliferative disorder of Langerhans cells that affects the lungs and other organs of cats, LCH involving a single organ system has not been documented in cats, to our knowledge. Herein we describe a case of pancreatic LCH in a 9-y-old castrated male Domestic Shorthaired cat that was evaluated for possible renal transplantation. The cat was hypoglycemic, hyperinsulinemic, and azotemic. Ultrasound examination revealed a diffusely enlarged, normoechoic pancreas. The cat was euthanized because of severe renal azotemia and the possibility of pancreatic neoplasia. Grossly, the pancreas was enlarged, and both kidneys were pale white, firm, and had irregular capsular surfaces. Histologically, the pancreas was expanded with interlobular, intraparenchymal, and ductal clusters of round-to-polygonal cells admixed with fibrous connective tissue and scattered lymphocytes. Infiltrating cells had a moderate amount of eosinophilic cytoplasm, round-to-indented nuclei with finely stippled chromatin and 1 or 2 nucleoli, and were strongly immunoreactive for CD18, ionized calcium-binding adapter molecule 1, and e-cadherin. The morphologic and immunohistochemical features of the pancreatic changes were consistent with single-system LCH.

Key words: cats; feline; Langerhans cell histiocytosis; pancreas.

Langerhans cells (LCs) are dendritic cells (DCs) that arise in bone marrow and reside within the epidermis and visceral epithelium.[10] Together with interstitial DCs, which reside mainly in the perivascular spaces of multiple organs, LCs are antigen-presenting cells that play a crucial role in the regulation of the T-cell immune response within regional lymph nodes.[10,11] Disorders associated with LC proliferation are referred to as Langerhans cell histiocytosis (LCH), have been described in human and veterinary medicine,[1,3,7,11] and are characterized by tissue infiltration with LCs exhibiting various degrees of pleomorphism.[1,3,7,11] The underlying pathogenesis of LCH is poorly understood. Although clinical and molecular evidence favors neoplastic transformation rather than functional deregulation of LCs,[7,9] as suggested by the fact that subsets of LCH have an aggressive behavior and have been shown to represent a clonal expansion of LCs, other cases are clinically benign and regress after treatment has taken place, suggesting a reactive disorder.[1,3,7]

Human LCH occurs mainly in children and can be classified as single-system or multisystem LCH.[1,7] Single-system LCH causes single or multiple lesions in one organ system, especially bone, skin, or lymph nodes,[1,7] whereas multisystem LCH is characterized by lesions in 2 or more organ systems, mainly skin, bone, pituitary gland, lymph nodes, liver, bone marrow, spleen, and lungs.[7] In veterinary medicine, diseases associated with LC proliferation include pulmonary LC histiocytosis (PLCH) in cats, as well as cutaneous histiocytoma and cutaneous LCH in dogs.[11] Feline PLCH is an uncommon disorder that affects mainly older cats and frequently causes death or euthanasia because of progressive respiratory failure.[3] The disease is similar to human PLCH, a multisystem LCH of adult individuals also characterized by lung lesions with minor involvement of other organs.[15] PLCH in humans is associated with tobacco smoke or other environmental and genetic factors, and prognosis is good once treatment has taken place.[15] PLCH in cats is considered primarily a pulmonary disease, but secondary lesions have been described in organs such as lymph nodes, pancreas, kidneys, and liver.[3,11] Single-system LHC has not been documented in cats, to our knowledge. Herein we describe a case of feline pancreatic LCH with morphologic features consistent with those described in cases of human single-system LHC.[1,7]

A 9-y-old castrated male Domestic Shorthaired cat was evaluated for possible renal transplantation. Seventy days prior to admission, the cat had a normal serum biochemistry

Departments of Pathology and Athens Veterinary Diagnostic Laboratory (Rissi, Brown), Veterinary Biosciences and Diagnostic Imaging (Gendron), and Small Animal Medicine and Surgery (Good, Lane, Schmiedt), College of Veterinary Medicine, University of Georgia, Athens, GA.

[1]Corresponding author: Daniel R. Rissi, Department of Pathology and Athens Veterinary Diagnostic Laboratory, College of Veterinary Medicine, University of Georgia, Athens, GA 30602. rissi@uga.edu

profile and complete blood count, but became lethargic and inappetent 10 d before admission. Complete blood work and biochemistry at that time revealed azotemia (creatinine 1,060 µmol/L, reference interval [RI]: 53–106 µmol/L; urea 46.4 mmol/L, RI: 2.9–8.2 mmol/L) and hyperphosphatemia (phosphorus 5.20 mmol/L, RI: 0.74–1.52 mmol/L). Blood glucose was normal (5.49 mmol/L, RI: 3.9–6.1 mmol/L). Blood pressure was also normal. A Doppler blood pressure reading was 116 mm Hg. ELISA for feline leukemia virus and feline immunodeficiency virus was negative. Urine culture did not yield any growth, and the urine protein-to-creatinine ratio was 0.7; urine specific gravity was not measured. Abdominal radiographs revealed an enlarged right kidney and a small left kidney. Intravenous fluid therapy did not result in significant improvement in the azotemia. An esophagostomy tube was placed, and the cat was given a slurry diet.

At admission, the cat was obese (6.6 kg) and lethargic, but alert, eupneic, and responsive. Body temperature was 37.4°C (99.3°F), pulse rate was 160 bpm, and blood pressure was 100 mm Hg. Complete bloodwork at time of admission revealed persistent azotemia (creatinine 707 µmol/L), metabolic acidosis (pH 7.2), and hypoglycemia (2.61 mmol/L). The packed cell volume was 0.46 L/L (RI: 0.35–0.45 L/L), and the urine specific gravity was 1.010 (RI: >1.035). The cat was judged to be ~7% dehydrated. Blood was obtained for an insulin-to-glucose ratio prior to correcting the hypoglycemia, which revealed that the cat was hypoglycemic (glucose 2.28 mmol/L) and hyperinsulinemic (insulin 166 pmol/L, RI: 14–140 pmol/L). A baseline cortisol was elevated (2,760 nmol/L, RI: 140–690 nmol/L). An intravenous (IV) catheter was placed, and the cat was given a 75-mL IV bolus of lactated Ringer solution (LRS) and started on 18 mL/h of LRS with 2.5% dextrose. Following the addition of dextrose to the IV fluids, hourly blood glucose measurements were <1.11, 3.72, 3.11, and 4.50 mmol/L, at which time the dextrose supplementation was increased to 5%. A slurry diet was continued through the esophagostomy tube every 4 h.

On ultrasound examination (Fig. 1; Toshiba Xario XG; Toshiba America Medical Systems, Tustin, CA), the body and left lobes of the pancreas were moderately enlarged, up to 15.5 mm for the body (RI: 4.7–9.52 mm) and up to 14.3 mm for the left limb (RI: 3.4–9.0 mm).[5] In these areas, the pancreas had undulant and irregular margins, and was surrounded by hyperechoic mesentery. The pancreas was normoechoic, isoechoic to the liver, and had a grainy echotexture. The right pancreatic lobe was unremarkable. The cat remained dependent on IV dextrose supplementation to maintain euglycemia, and the azotemia worsened (creatinine 884 µmol/L). The hydration status was improved, although metabolic acidosis remained (pH 7.2), and the cat developed hyperkalemia (potassium 6.20 mmol/L, RI: 3.5–5 mmol/L).

Triple-phase computed tomographic angiography (Somatom Sensation; Siemens, Munich, Germany) of the abdomen was performed to further evaluate the pancreas for the presence of nodules, because insulinoma was considered to be a potential cause of persistent hypoglycemia.[13] Images were acquired in ventral recumbency on the bed of a 64-slice helical computed tomography (CT) scanner, using 120 kVp, 200 mAs, a spiral pitch factor of 0.8, and reconstructed into 0.6-mm slices. Pre-contrast, arterial, and delayed post-contrast phases were performed. The contrast medium consisted of 350 mg/mL of iohexol (Omnipaque 350; GE Healthcare, Princeton, NJ), 600 mg/kg IV via pressure injector at a rate of 5 mL/s. The pancreas (Fig. 2) had undulant margins, and the tip of the left pancreas was moderately thickened (12-mm thick) and nodular in appearance. Mean attenuation was normal before administration of contrast (47 HU) and in mixed arterioportal (115 HU) and delayed (85 HU) phases,[14] with a slightly heterogeneous enhancement pattern on arterial phase images. Surrounding the body and left lobe of the pancreas were countless small soft tissue density nodules within the mesenteric fat. A single pancreaticoduodenal lymph node was present, 5.6 mm in width (RI: 2–8 mm),[12] which showed heterogeneous enhancement. To test the cat's dependence on dextrose glucose supplementation, dextrose was removed from the IV fluids, and within 2 h the glucose fell from 7.05 mmol/L to 3.03 mmol/L. The cat was not considered an acceptable candidate for renal transplantation given the unexplained persistent hypoglycemia and the possibility of pancreatic neoplasia. Given the poor prognosis, the cat was euthanized and subjected to autopsy.

Grossly, the pancreas was mildly enlarged, and an 8-mm diameter, soft tan nodule (pancreaticoduodenal lymph node) was present at the margin of the pancreatic neck. The right kidney was swollen (5 × 3 × 3 cm), and the left kidney was small (2.8 × 3 × 2 cm); both were pale white, firm, and had irregular capsular surfaces. No other changes were present. Fresh samples of spleen, liver, and lung were submitted for aerobic bacterial culture, which yielded light growth of *Escherichia coli* (liver and lung), *Chryseobacterium indologenes* (spleen), and *Acinetobacter* spp. (spleen). Routine samples of multiple organs (including pancreatic head, body, and tail) were collected, fixed in 10% neutral-buffered formalin, routinely processed for histology, and stained with hematoxylin and eosin.

Histologically, the exocrine pancreas was expanded with interlobular, parenchymal, and ductal accumulations of moderate-to-large numbers of round histiocytic cells arranged in cords or small clusters (Fig. 3). The affected interlobular tissues were also expanded by fibrous connective tissue, which often created a nodular appearance to the exocrine pancreas (Fig. 4). Infiltrating histiocytic cells (Fig. 5) had a moderate amount of eosinophilic cytoplasm and round-to-indented nuclei with finely stippled chromatin and 1 or 2 nucleoli. No mitoses were seen in ten 400× fields. Accumulations of lymphocytes were scattered throughout. The small nodules within the mesenteric fat observed via CT were foci of mesenteric fat admixed with neutrophils adjacent to the pancreas.

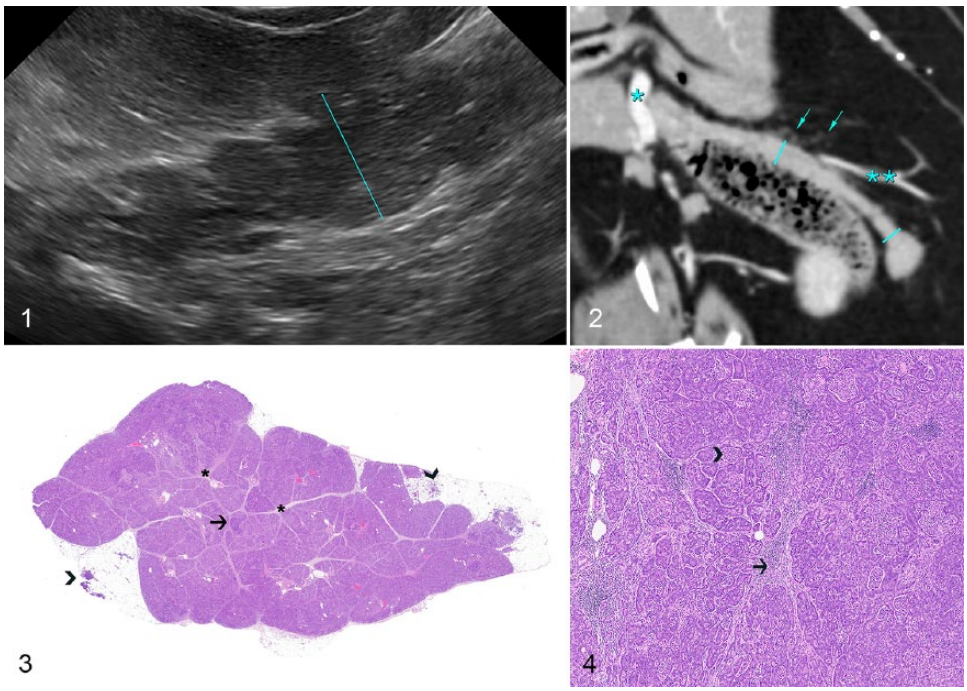

Figures 1–4. Pancreatic Langerhans cell histiocytosis in a cat. **Figure 1**. Sagittal ultrasound image of the body of the pancreas. At the level indicated by the calipers, the pancreatic body measures 15.2 mm. The body and left lobe of the pancreas are characterized by undulant margins and moderate enlargement but normal echogenicity. **Figure 2**. Triple-phase computed tomographic angiography, dorsal oblique reconstruction, arterial phase, soft tissue window (right is left on the image). The left lobe of the pancreas (calipers) conforms to the transverse colon. Nodular enlargement of the tip of the left lobe is present. The mesentery surrounding the pancreas contains fine, dense soft tissue foci (arrows). Portal vein (*) and splenic vein (**) are indicated for reference. **Figure 3**. Low magnification of a cross-section of the pancreas evidencing widespread expansion of the interlobular spaces (asterisks) and distortion of the adjacent parenchyma, with scattered nodular areas throughout (arrow). The small soft tissue density nodules within the mesentery observed via computed tomographic angiography were areas of fat necrosis and infiltration with neutrophils (arrowheads). H&E. **Figure 4**. Round histiocytic cells, lymphocytes, and fibrous connective tissue expand and disrupt the interlobular spaces (arrow), and solid clusters of histiocytic cells infiltrate the pancreatic parenchyma throughout (arrowhead). H&E.

A focal area of mucosal loss and necrosis, with moderate numbers of neutrophils admixed with fibrin, was present in the small intestine; the inflammation extended to the submucosa and into the outer and inner muscle layers, where it was centered on blood capillaries that were often occluded by fibrin thrombi. Scattered neutrophils were distributed throughout the pulmonary alveolar septa and rarely within the splenic red pulp. Both kidneys had linear areas of cortical and corticomedullary tubular loss with fibrosis and accumulation of free and intra-macrophagic lipid vacuoles admixed with neutrophils, lymphocytes, and plasma cells. Neutrophils were also present within vasa recta. Lymphocytes and plasma cells were scattered within the medulla. No other changes were present in other organs. Tissue sections of pancreas, intestine, spleen, and lung were stained with Brown and Brenn Gram method, Grocott–Gomori methenamine silver stain, and periodic acid–Schiff, but no organisms were detected.

Immunohistochemistry (IHC) for CD18 (mouse monoclonal, 1 in 10 dilution for 60 min; Dr. Peter Moore, University of California, Davis, CA), ionized calcium-binding adapter molecule 1 (Iba1; rabbit polyclonal antibody, 1 in 8,000 dilution for 60 min; Wako, Richmond, VA), e-cadherin (mouse monoclonal, 1 in 500 dilution for 60 min; BD Biosciences, Sparks, MD), multiple myeloma oncogene 1/interferon regulatory factor 4 MUM1 (MUM1; rabbit monoclonal antibody, 1 in 50 dilution for 60 min; Biocare Medical, Pacheco, CA), pan-cytokeratin (AE1/AE3, mouse monoclonal, 1 in 100 dilution for 90 min; Biocare Medical), insulin (guinea pig polyclonal, 1 in 2,000 dilution for 30 min; MilliporeSigma, St. Louis, MO), glucagon (rabbit polyclonal, 1 in 1,000 dilution for 60 min; Dako, Carpinteria, CA), and synaptophysin (mouse monoclonal, 1:600 dilution at 60 min; Biogen, Cambridge, MA) was performed on multiple sections of pancreas. In addition, IHC for feline infectious peritonitis virus (FIP; mouse monoclonal antibody, 1:600 dilution at 60 min; Custom Monoclonals International, West Sacramento, CA) was performed on sections of pancreas, liver, spleen, and small intestine. Infiltrating histiocytic cells throughout the pancreas were strongly immunoreactive for CD18 (Fig. 6), Iba1 (Fig. 7), and e-cadherin (Fig. 8), and negative for the other markers. Throughout the pancreatic parenchyma, exocrine cells were immunoreactive for e-cadherin and AE1/AE3, and the endocrine tissue was immunoreactive for insulin, glucagon, and synaptophysin. FIP IHC was negative.

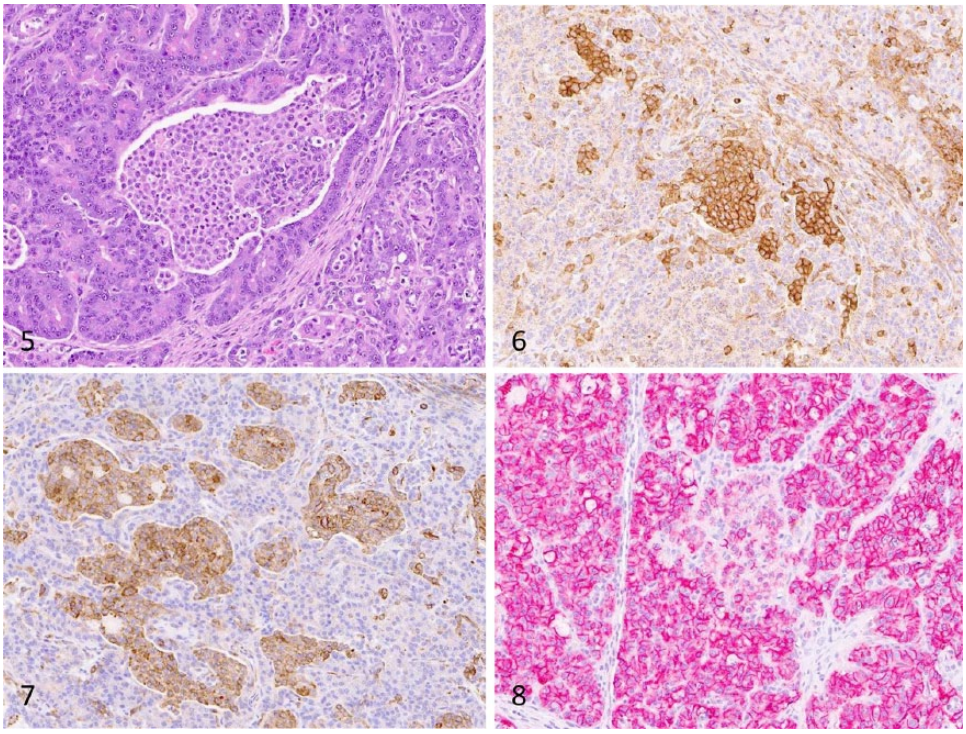

Figures 5–8. Pancreatic Langerhans cell histiocytosis in a cat. **Figure 5**. Infiltrating histiocytic cells have a moderate amount of eosinophilic cytoplasm and round-to-indented nuclei with finely stippled chromatin and 1 or 2 nucleoli. H&E. **Figure 6**. Infiltrating histiocytic cells exhibit strong membranous immunoreactivity for CD18. **Figure 7**. Infiltrating histiocytic cells exhibit strong cytoplasmic immunoreactivity for Iba1. **Figure 8**. Infiltrating histiocytic cells exhibit moderate membranous immunoreactivity for e-cadherin. Strong e-cadherin expression is present throughout the surrounding exocrine pancreas.

The morphologic and IHC features in our case are consistent with those of single-system LCH described in human medicine.[1] Similar pancreatic changes have been reported in 2 of 3 affected cats described in the veterinary medical literature,[3] but were considered secondary to primary pulmonary involvement, as reported in human cases of PLCH.[3] A detailed clinical history and an autopsy with systematic histologic examination of multiple organs, including lungs, were key features that allowed for a diagnosis of single-system pancreatic LCH in our case.[1,3,11] All 3 originally described cases of feline LCH,[3] as well as 4 additional cases mentioned in a review article,[11] have been characterized as primarily pulmonary in origin and, to our knowledge, single-system LHC has not been documented in cats. Single-system LCH in humans is typically benign and characterized by one or more lesions in one organ system, more commonly bone and skin.[1,7]

The pathogenesis of LCH is not fully understood, but studies have identified a number of oncogenic mutations in affected human patients, supporting the hypothesis that LCH represents myeloid neoplasia rather than a reactive disorder.[9] In fact, LCH is currently defined as an inflammatory myeloid neoplasm in the revised 2016 Histiocyte Society classification.[9] In addition, PLCH in humans is strongly correlated with smoking or less often other environmental factors, indicating that other mechanisms may also play a role in the development of the disease.[1,7,9] The pathogenesis of LCH has not been elucidated in veterinary medicine, and the development of molecular techniques to assess clonality and detect possible mutations is needed to provide insights into the development of this enigmatic disorder.[3]

Hyperinsulinemia was considered the cause of the hypoglycemia in our case, but the mechanism underlying the increased insulin production could not be determined. Given the clinical history and pathology findings, the most likely causes of hyperinsulinemia include a functional pancreatic tumor (insulinoma), endocrine cell proliferation secondary to widespread pancreatic injury, and septicemia.[2,6,8] No evidence of neoplasia was observed in multiple sections of pancreas and other organs. Widespread islet cell proliferation (nesidioblastosis) has been described rarely as a response to pancreatic injury in veterinary medicine,[8] and was considered because of the widespread parenchymal damage caused by LC infiltration and fibrosis; however, no morphologic changes consistent with islet cell proliferation were observed in the endocrine pancreas.[8] Bacterial growth from spleen, liver, and lung, together with the presence of neutrophils within the pulmonary alveolar septa and splenic red pulp, support the role of septicemia as a result of intestinal damage as the main possibility for hyperinsulinemia. However, the cat was cardiovascularly stable and afebrile ~24 h before

death, which makes this possibility questionable. Intestinal ulceration was attributed to the severe azotemia of chronic renal disease.[4]

The diagnosis of LCH in human and veterinary medicine is based on histologic features and confirmed with IHC.[3,7] The robust immunoreactivity of the infiltrating round cells with CD18 and Iba1 in our case was supportive of their histiocytic origin.[3,11] Further, e-cadherin is expressed mainly by epithelial cells, but also by melanocytes and LCs.[11] Given that e-cadherin immunolabeling has not been reported in other histiocytic disorders of dogs and cats, its positivity is highly supportive of LC origin.[3,11] In feline LCH, e-cadherin expression was reportedly reduced in extra-pulmonary lesions, which was attributed to down-regulation of e-cadherin associated with distant migration from the lung.[3] That feature could not be assessed in our case because of the single-site location of the lesions. Although other antibodies, such as CD1a and langerin, are also expressed exclusively by LCs and could be used to further confirm the diagnosis of feline LCH, their availability and use is limited because the antibodies cannot be used on formalin-fixed tissues or are not available to be used on feline tissues, respectively.[3] Although rare, LCHs should be suspected in cases of diffuse enlargement of the pancreas.

Declaration of conflicting interests

The authors declare no potential conflicts of interest with respect to the research, authorship, and/or publication of this article.

Funding

The authors declared that they received no financial support for their research and/or authorship of this article.

References

1. Abla O, et al. Langerhans cell histiocytosis: current concepts and treatments. Cancer Treat Rev 2010;36:354–359.
2. Breitschwerdt EB, et al. Hyperinsulinemic hypoglycemia syndrome in 2 dogs with bartonellosis. J Vet Intern Med 2014;28:1331–1335.
3. Busch MD, et al. Feline pulmonary Langerhans cell histiocytosis with multiorgan involvement. Vet Pathol 2008;45:816–824.
4. Cianciolo RE, et al. Chapter 4. Urinary system. In: Maxie MG, ed. Jubb, Kennedy, & Palmer's Pathology of Domestic Animals. 6th ed. Vol. 2. St. Louis, MO: Elsevier, 2016:376–464.
5. Etue SM, et al. Ultrasonography of the normal feline pancreas and associated anatomic landmarks: a prospective study of 20 cats. Vet Radiol Ultrasound 2001;42:330–336.
6. Ferguson DC, et al. Endocrine system. In: Latimer KS, ed. Duncan and Prasse's Veterinary Laboratory Medicine: Clinical Pathology. 5th ed. Ames, IA: Wiley, 2011:295–329.
7. Jezierska M, et al. Langerhans cell histiocytosis in children—a disease with many faces. Recent advances in pathogenesis, diagnostic examinations and treatment. Postepy Dermatol Alergol 2018;35:6–17.
8. Katsuta O, et al. Abnormal proliferation of pancreatic endocrine cells in Beagle dogs. J Toxicol Pathol 1992;5:67–76.
9. Kobayashi M, Tojo A. Langerhans cell histiocytosis in adults: advances in pathophysiology and treatment. Cancer Sci 2018;109:3707–3713.
10. Merad M, et al. Origin, homeostasis and function of Langerhans cells and other langerin-expressing dendritic cells. Nat Rev Immunol 2008;8:935–947.
11. Moore PF. A review of histiocytic diseases of dogs and cats. Vet Pathol 2014;51:167–184.
12. Perlini M, et al. Computed tomographic appearance of abdominal lymph nodes in healthy cats. J Vet Intern Med 2018;32:1070–1076.
13. Robben JH, et al. Comparison of ultrasonography, computed tomography, and single-photon emission computed tomography for the detection and localization of canine insulinoma. J Vet Intern Med 2005;19:15–22.
14. Secrest S, et al. Triple phase computed tomography of the pancreas in healthy cats. Vet Radiol Ultrasound 2018;59:163–168.
15. Vassallo R, et al. Pulmonary Langerhans'-cell histiocytosis. N Engl J Med 2000;342:1969–1978.